ARCHIVES OF ACOUSTICS Vol. **48**, No. 2, pp. 231–234 (2023), doi: 10.24425/aoa.2023.145228

Research Paper

Effect of Rotation on the Piezoelectric Wave Impedance Characteristics

Xiaoguang YUAN*, Chaoyu HAO, Quan JIANG

School of Transportation and Civil Engineering, Nantong University
Nantong, China

*Corresponding Author e-mail: xgyuan@gmail.com

(*received May 24, 2022; accepted November 20, 2022*)

The dependence of piezoelectric wave impedance on the rotation speed is investigated theoretically and numerically. The Coriolis force due to rotation is introduced into the piezoelectric motion equations, which is solved by the harmonic plane wave solution. It is shown that the wave impedance variations of longitudinal and transverse waves due to rotation are clearly different. The longitudinal wave impedance continuously increases with a small rotation ratio and one transverse wave impedance is almost irrespective of a rotation ratio. In contrast, the rotation applies a big impact on the other transversal wave impedances in the piezoelectric crystal which decreases monotonically with the rotation speed. Such characteristics are significant in piezoelectric transducers and sensors.

Keywords: wave impedance; Coriolis acceleration; piezoelectric crystal; wave velocity.

1. Introduction

Under ordinary conditions, the solid-to-gas ultrasonic transmission encounters the problem of large acoustic impedance mismatch and makes it difficult to transfer the ultrasonic wave energy commutatively.

It is due to the close to zero transmission coefficient of an equation expression in the form of wave impedance, for the linear wave field, defined by dividing wave pressure with the particle velocity at some position. In an unbounded medium, the wave impedance is independent of the position and is numerically equal to the product of density and wave velocity, i.e., $Z = \rho v$ [$\text{Pa}\cdot\text{sec}\cdot\text{m}^{-1}$] known as "the specific or characteristic wave impedance".

Consequently in the gas sensor field, it is difficult to use directly the piezoelectric crystal device to detect gas features, etc., (LYNNWORTH, 1965). One may turn to the medium of slower density, like P(VDF/TrFE) (TAKAHASHI, OHIGASHI, 2009), or other technologies, i.e., adding the chemical reaction film (WANG *et al.*, 2021), the transition layer (SURAPPA *et al.*, 2018), or a resonance cavity (DONG *et al.*, 2003) for the specific kind of gas.

In essence, the fundamental solution is to slow the piezoelectric wave impedance in order to interact between solid and gas, which is a problem of equal scientific and practical significance as well as helpful for the above technology.

Unfortunately no one attempts to slow the wave velocity to obtain smaller wave impedance in the acoustic field. In the field of solid mechanics, the authors of references (YUAN, 2016; 2019; YUAN, JIANG, 2017; YUAN *et al.*, 2016; 2020; YUAN, LI, 2015a; 2015b) investigated the propagation, refection and transmission processes of bulk waves in the rotating piezoelectrics and pyroelectrics, from which it is found that the Coriolis force due to rotation can change the bulk wave velocities.

Accordingly, the objective of the present study consists in investigating the piezoelectric wave impedance characteristics in the acoustic field using the Coriolis force.

2. Problem formulation and results

The object of investigation is an infinite piezoelectric medium (Fig. 1), in which the computational coordinates (x_1, x_2, x_3), n_i, θ, and Ω_i are indicated.

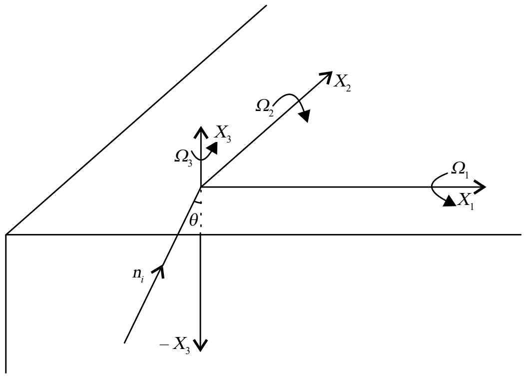

Fig. 1. Wave propagation in the infinite piezoelectric crystal: n_i wave propagation vector, θ wave propagation angle, Ω_i rotation speed vector.

We introduce the Coriolis force K_i due to rotation (Suchkov *et al.*, 2011; Yuan, Jiang, 2017)

$$K_i = 2\rho\varepsilon_{irk}\Omega_r \frac{\partial u_k}{\partial t} \tag{1}$$

to the piezoelectric motion equation and obtain:

$$\begin{gathered} C_{ijkl}u_{k,li} + e_{kij}\phi_{,ki} = \rho\left[\frac{\partial^2 u_j}{\partial t^2} + 2\varepsilon_{jik}\Omega_i\frac{\partial u_k}{\partial t}\right], \\ -\epsilon_{ij}\phi_{,ji} + e_{ikl}u_{k,li} = 0, \end{gathered} \tag{2}$$

where ρ represents mass density, t is time, u_j is the displacement vector, ϕ is the electric potential, ε_{jik}, C_{ijkl}, e_{kij}, ϵ_{ij} indicate the tensors of permutation, elasticity, piezoelectricity, and permittivity constant. Ω_i is the rotation speed vector whose unit is the same with the wave frequency ω, so the dimensionless quantity of the rotation ratio $\eta_i = \Omega_i/\omega$ is used in the following.

Without loss of generality, we seek a harmonic plane wave solution in the form:

$$\{u_1, u_2, u_3, \phi\} = \{U_1, U_2, U_3, \Phi\}\, e^{I\omega(s_i x_i - t)}, \tag{3}$$

where s_i is the slowness vector, ω is the wave frequency and I equals to $\sqrt{-1}$. (U_i, Φ) are amplitudes of the displacement and the electric potential $\{u_1, u_2, u_3, \phi\}$.

After substituting Eq. (3) in (2), we obtain:

$$\begin{bmatrix} s_l s_i \overset{\circ}{C}_{irkl} - \rho\delta_{rk} - 2I\varepsilon_{rik}\eta_i & s_j s_i \overset{\circ}{e}_{jir} \\ s_l s_i \overset{\circ}{e}_{ikl} & -s_j s_i \overset{\circ}{\epsilon}_{ij} \end{bmatrix} \begin{Bmatrix} U_k \\ \Phi \end{Bmatrix} = \begin{Bmatrix} \mathbf{0} \\ 0 \end{Bmatrix}, \tag{4}$$

where

$$s_i = n_i/v, \tag{5}$$

n_i denotes the wave propagation vector (Fig. 1), and v is the wave velocity. Replacing the slowness vector in Eq. (4) by Eq. (5) and considering the condition of non-vanishing (U_i, Φ), we obtain an associated characteristic polynomial equation about v.

As an computational example, the material parameters of piezoelectric medium lithium niobate are listed in Table 1 and their Voigt notation matrices were presented in (Ledbetter *et al.*, 2004).

The computation was carried out under the following conditions: the rotation ratio $\eta_i = \frac{\Omega_i}{\omega}$, in which the subscript i indicates that the rotation axis is the x_i axis; ω – wave frequency – (= 1 MHz) and the wave propagation vector of $(\sin\theta,\ 0,\ \cos\theta)$ lies on the x_1–x_3 plane without loss of generality.

According to the computation results of Eqs. (4) and (5), it is found that when the rotation ratio about any axis is above 0.00235, the real part of velocity of the longitudinal wave vanishes, which implies that it does not propagate and becomes the harmonic form of vibration in the angular frequency ω.

Therefore, in Fig. 2, a dimensionless quantity of $Z(\eta_i = 0.002)/Z_0$ is defined as the ratio between wave impedances in the case of $\eta_i = 0.002$ and the case of $\eta_i = 0$.

Figure 2 exhibits the variations of wave impedance ratios of L, T1, and T2 waves as function of the propagation angle θ in the case of $\eta_1, \eta_2, \eta_3 = 0.002$, respectively. We see that the increases of L wave impedance due to rotation are different with θ especially in the case of η_3; in contrast, the wave impedance of T2 wave drops remarkably below the half of the case of without rotation almost at any θ. The feature of T1 wave is similar to T2 wave in the case of η_2 and shows a big change with θ in the case of η_3.

Table 1. Lithium niobate ($LiNbO_3$) material parameters (James, 1975).

Elasticity tensor C_{ij} [GPa]	C_{11}	C_{33}	C_{44}	C_{12}	C_{13}	C_{14}
	203	245	60	53	75	9
Piezoelectric stress tensor e_{ij} [C/m^2]	e_{15}	e_{22}	e_{31}	e_{33}		
	3.7	2.5	0.2	1.3		
Normalized permittivity tensor ϵ_{ij}/ϵ_0	ϵ_{11}/ϵ_0	ϵ_{33}/ϵ_0				
	44	29				
Vacuum permittivity ϵ_0 [F/m]	8.854×10^{-12}					
Density ρ [kg/m^3]	4700					

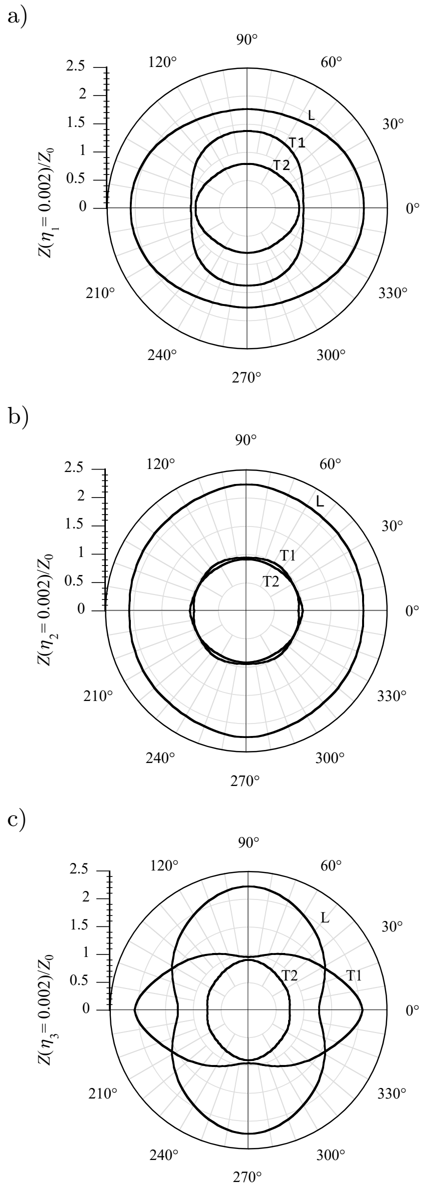

Fig. 2. Wave impedance ratio variations with wave propagation angle: a) indicates the case of rotation about the axis x_1; b) the axis x_2; c) the axis x_3. L represents the longitudinal wave, and T1, T2 the transverse waves.

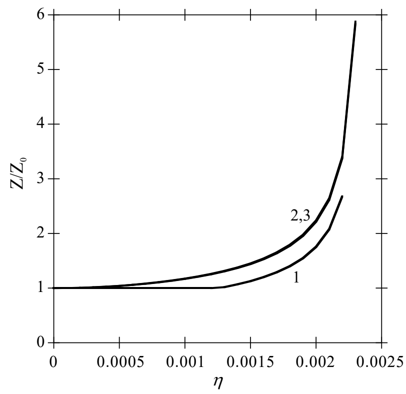

Fig. 3. Wave impedance ratio of L wave rotating about x_1, x_2, and x_3 axis, 1 indicates axis x_1, 2 – x_2, 3 – x_3.

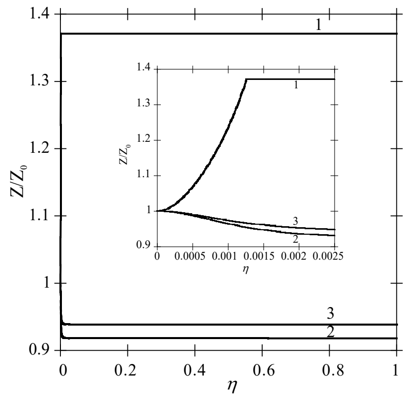

Fig. 4. Wave impedance ratio of T1 wave rotating about x_1, x_2, and x_3 axis, 1 indicates axis x_1, 2 – x_2, 3 – x_3.

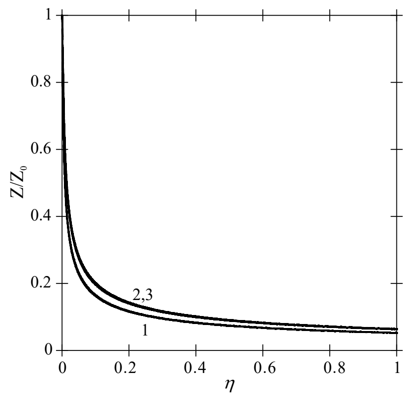

Fig. 5. Wave impedance ratio of T2 wave rotating about x_1, x_2, and x_3 axis, 1 indicates axis x_1, 2 – x_2, 3 – x_3.

Next, setting $\theta = \frac{\pi}{2}$, we can investigate the wave impedances as a function of the rotation ratio as shown in Figs. 3, 4, and 5.

The L wave only exists for a low rotation ratio, i.e., $\eta < 0.00235$. The changes of L wave impedance initially are not obvious and then become large especially in the case of rotating about x_2, x_3 as shown in Fig. 3.

Figure 4 shows the variation of the wave impedance ratio of T1 wave as a function of the rotation ratio. We see that T1 wave is not sensitive to rotation except for small η: the wave impedance ratio of η_1 grows rapidly to be in the vicinity of 1.4, and then remain unchanged; in the cases of η_2 and η_3 their wave impedances are similar.

From Fig. 5, we see that the wave impedance ratio of T2 wave is a monotone decreasing function of the rotation ratio of η_1, η_2, and η_3.

Analyzing the curves of Figs. 3–5, we assert the following: the numerical results presented indicate that the rotation influence on wave impedance is remarkable; however, wave impedance variations of longitudinal and transverse waves due to rotation differ distinctly. For instances, the longitudinal wave impedance continuously increases within a small rotation ratio.

For transverse waves, one transverse wave impedance is almost irrespective of the rotation ratio η except for the small interval of the rotation ratio η, out of which it acquires a horizontal line irrespective of the rotation ratio. On the other hand, T2 wave impedance of the other transverse wave between the interval of η = 0 and 1 drops monotonically (Fig. 5). When the rotation ratio η is 1, its wave impedance decreases by 95%. Thus, the application of this wave of a transverse mode is particularly advantageous to acquire small wave impedance in the associated technologies.

3. Conclusions

The wave impedances in the rotating piezoelectric crystal are studied theoretically and numerically. We note that, characteristically, the Coriolis force induced by rotation is justified to significantly alter wave impedances, particularly to that of the transverse wave. As the rotation increases, the wave impedance of T2 wave become small monotonically, this, in essence, increases the transmission coefficient and accordingly enhances the interaction between gas and the piezoelectric crystal. Such distinct attributes are very valuable from the viewpoint of the practical utilization, i.e., in the acoustic electronic devices like the piezoelectric transducer and acoustic sensors, which have never been reported and put into application before.

Acknowledgments

The author expresses his appreciation to Jiangsu Province Natural Science Foundation (BK20191450), Jiangsu Province Higher Education Institutions Natural Science Foundation (18KJB130004), and Nantong Basic Science Foundation (JC22022101).

Ethical standards and conflict of interest

The named authors confirm that all the research meets the ethical guidelines, including compliance with the legal requirements of the country of study. The authors declare the following financial interests/personal relationships which may be considered as potential competing interests: Xiaoguang Yuan reports financial support was provided by Jiangsu Province Natural Science Foundation and Jiangsu Province Higher Education Institutions Natural Science Foundation.

References

1. Dong S., Bai F., Li J.-F., Viehland D. (2003), A piezoelectric-sound-resonance cavity for hydrogen gas detection, *IEEE Transactions on Ultrasonics, Ferroelectrics, and Frequency Control*, **50**(9): 1105–1113, doi: 10.1109/tuffc.2003.1235322.
2. James B. (1975), Acoustic fields and waves in solids, volumes I and II: B.A. Auld. Published by J. Wiley and Sons, Ltd. 1973, Book review, *Applied Acoustics*, **8**(1): 72–73, doi: 10.1016/0003-682X(75)90008-0.
3. Ledbetter H., Ogi H., Nakamura N. (2004), Elastic, anelastic, piezoelectric coefficients of monocrystal lithium niobate, *Mechanics of Materials*, **36**(10): 941–947, doi: 10.1016/j.mechmat.2003.08.013.
4. Lynnworth L.C. (1965), Ultrasonic impedance matching from solids to gases, *IEEE Transactions on Sonics and Ultrasonics*, **12**(2): 37–48, doi: 10.1109/t-su.1965.29359.
5. Suchkov S.G., Nikolaevtsev V.A., Nikitov V. (2011), The influence of rotation on a phase deviation in surface acoustic wave devices, *Journal of Communications Technology and Electronics*, **56**: 1017, doi: 10.1134/S1064226911080110.
6. Surappa S., Tao M., Levent Degertekin F. (2018), Analysis and design of capacitive parametric ultrasonic transducers for efficient ultrasonic power transfer based on a 1-D lumped model, *IEEE Transactions on Ultrasonics, Ferroelectrics, and Frequency Control*, **65**(11): 2103–2112, doi: 10.1109/tuffc.2018.2866058.
7. Takahashi S., Ohigashi H. (2009), Ultrasonic imaging using air-coupled P(VDF/TrFE) transducers at 2 MHz, *Ultrasonics*, **49**(4): 495–498, doi: 10.1016/j.ultras.2008.10.020.
8. Wang B., Sun L., Schneider-Ramelow M., Lang K.-D., Ngo H.-D. (2021), Recent advances and challenges of nanomaterials-based hydrogen sensors, *Micromachines*, **12**(11): 1429, doi: 10.3390/mi12111429.
9. Yuan X. (2016), Effects of rotation and initial stresses on pyroelectric waves, *Archive of Applied Mechanics*, **86**(3): 433–444, doi: 10.1007/s00419-015-1038-z.
10. Yuan X. (2019), Electric bias dependence of piezoelectric wave reflection upon a rotating half-plane, *ZAMM – Journal of Applied Mathematics and Mechanics*, **99**(10): e201900021, doi: 10.1002/zamm.201900021.
11. Yuan X., Jiang Q. (2017), Reflection of plane waves from rotating pyroelectric half-space under initial stresses, *ZAMM – Journal of Applied Mathematics and Mechanics*, **97**(3): 365–374, doi: 10.1002/zamm.201500223.
12. Yuan X., Jiang Q., Yang F., (2016), Wave reflection and transmission in rotating and stressed pyroelectric half-planes, *Applied Mathematics and Computation*, **289**: 281–297, doi: 10.1016/j.amc.2016.05.016.
13. Yuan X., Li L. (2015a), Wave reflection and refraction in rotating and initially-stressed piezoelectric crystals, *Acta Mechanica*, **226**(10): 3243–3261, doi: 10.1007/s00707-015-1377-4.
14. Yuan X., Li L. (2015b), Waves in a rotating pyroelectric body, *Journal of Thermal Stresses* **38**(4): 399–414, doi: 10.1080/01495739.2015.1015838.
15. Yuan X., Shi Q., Cao Y. (2020), Constant electric bias dependence of wave propagation in a rotating piezoelectric crystal, *Acta Mechanica*, **231**(3): 1209–1215, doi: 10.1007/s00707-019-02596-4.